

# Electronic Supplementary Material to: Supplementary Material for Recent Near-surface Temperature Trends in the Antarctic Peninsula from Observed, Reanalysis and Regional Climate Model Data\*

Deniz BOZKURT<sup>1,2</sup>, David H. BROMWICH<sup>3</sup>, Jorge CARRASCO<sup>4</sup>, Keith M. HINES<sup>3</sup>,  
Juan Carlos MAUREIRA<sup>5</sup>, and Roberto RONDANELLI<sup>6,2</sup>

<sup>1</sup>*Department of Meteorology, University of Valparaíso, Valparaíso 2340000, Chile*

<sup>2</sup>*Center for Climate and Resilience Research (CR)2, Santiago 8320000, Chile*

<sup>3</sup>*Polar Meteorology Group, Byrd Polar and Climate Research Center,  
The Ohio State University, Columbus, OH 43210, USA*

<sup>4</sup>*Centro de Investigación GAIA Antártica, Universidad de Magallanes, Punta Arenas 6200000, Chile*

<sup>5</sup>*Center for Mathematical Modeling (CMM), University of Chile, Santiago 8320000, Chile*

<sup>6</sup>*Department of Geophysics, University of Chile, Santiago 8320000, Chile*

**ESM to :** Bozkurt, D., D. H. Bromwich, J. Carrasco, K. M. Hines, J. C. Maureira, and R. Rondanelli, 2020: Recent near-surface temperature trends in the Antarctic Peninsula from observed, reanalysis and regional climate model data. *Adv. Atmos. Sci.*, **37**(5), 477–493, <https://doi.org/10.1007/s00376-020-9183-x>.

---

**Table S1.** Temporal correlations and root-mean-square-differences of reanalyses and numerical simulations forced with ERA-Interim for the San Martin and Larsen Ice Shelf stations.

Station		ERA5	ERA-Interim	RACMO	PWRF-45	PWRF-15
San Martin	<i>r</i>	0.8	0.84	0.7	0.69	0.9
	RMSD (°C)	2.3	2.6	1.9	3.8	1.7
Larsen Ice Shelf	<i>r</i>	0.78	0.43	0.74	0.83	0.79
	RMSD (°C)	3	5.5	3.1	3.9	1.9

---

\* The online version of this article can be found at <https://doi.org/10.1007/s00376-020-9183-x>.

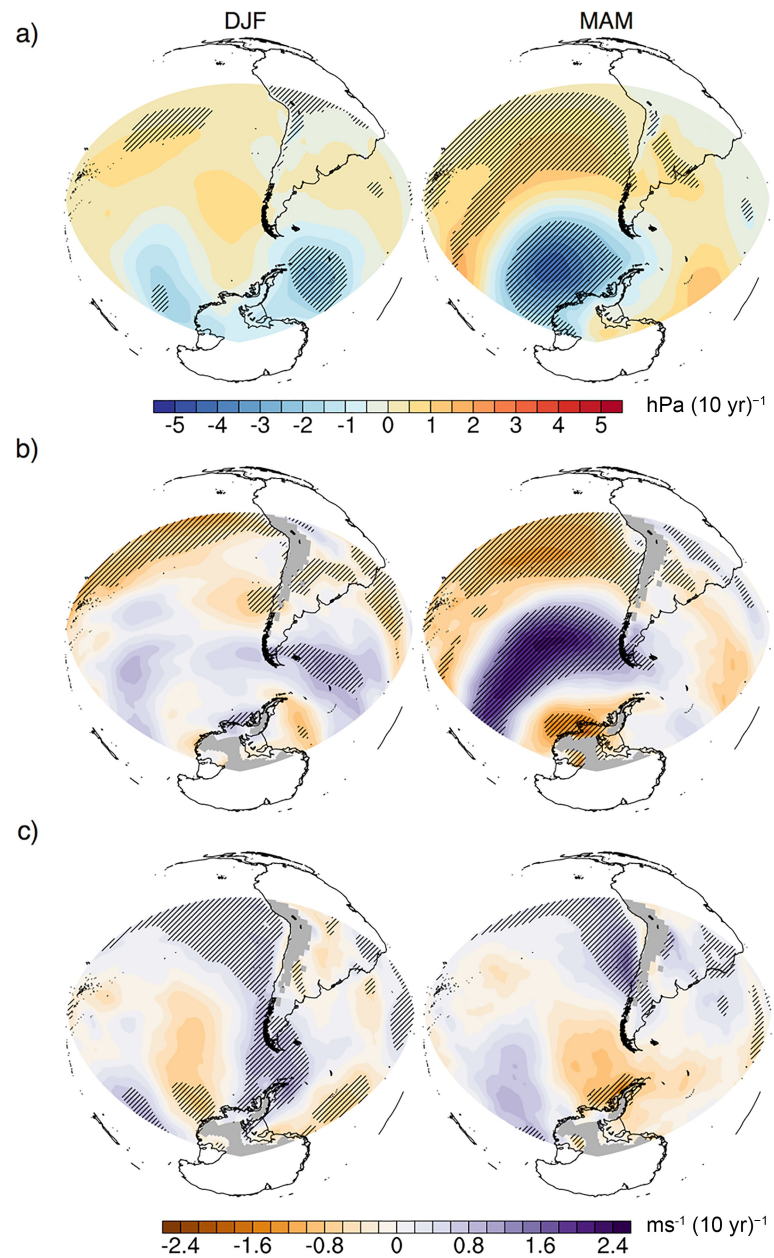


**Fig. S1.** Spatial distribution of summer (DJF, left plots) and autumn (MAM, right plots) trends in (a) mean sea level pressure, (b) 850-hPa zonal wind, and (c) 850-hPa meridional wind from ERA-Interim for the period 1991–2015. Regions with statistically significant trends at the 95% confidence level based on a two-tailed Student's *t*-test are hatched.

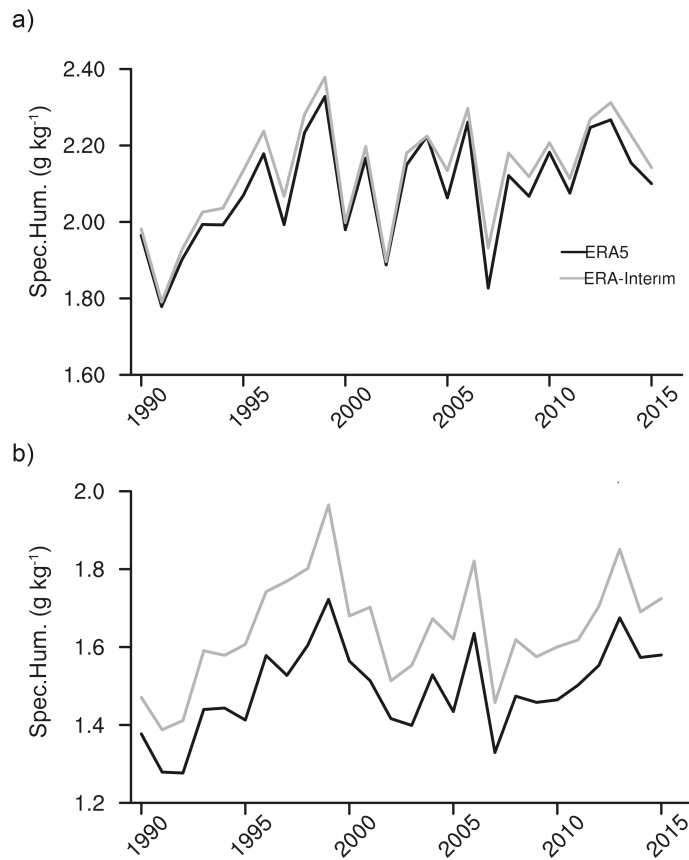


**Fig. S2.** Time series (1990–2015) of autumn (MAM) 850-hPa specific humidity averaged over the (a) windward and (b) leeward

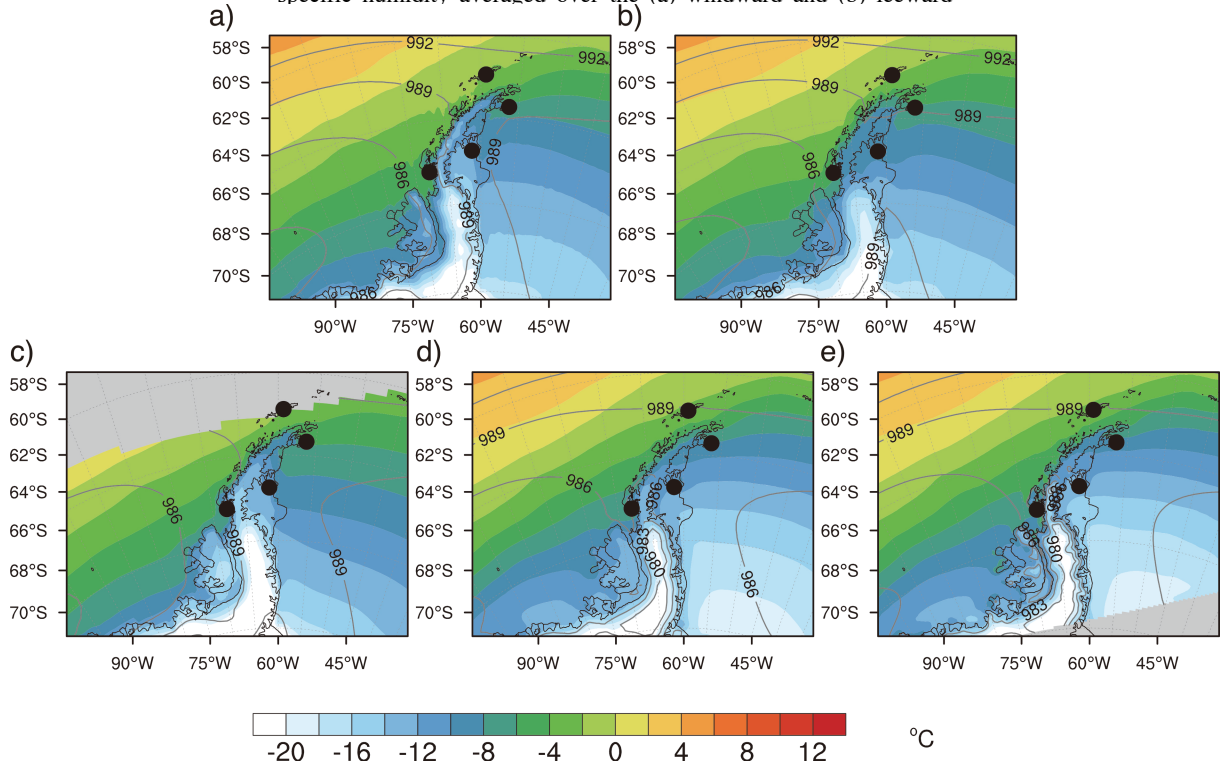


**Fig. S3.** Spatial distribution of mean annual near-surface air temperature (1991–2012) over the Antarctic Peninsula for (a) ERA5, (b) ERA-Interim, (c) RACMO, (d) PWRF-45, and (e) PWRF-15. Also included are contours for mean sea level pressure (interval: 3 hPa). The filled black circles show the locations of meteorological stations used in this study.

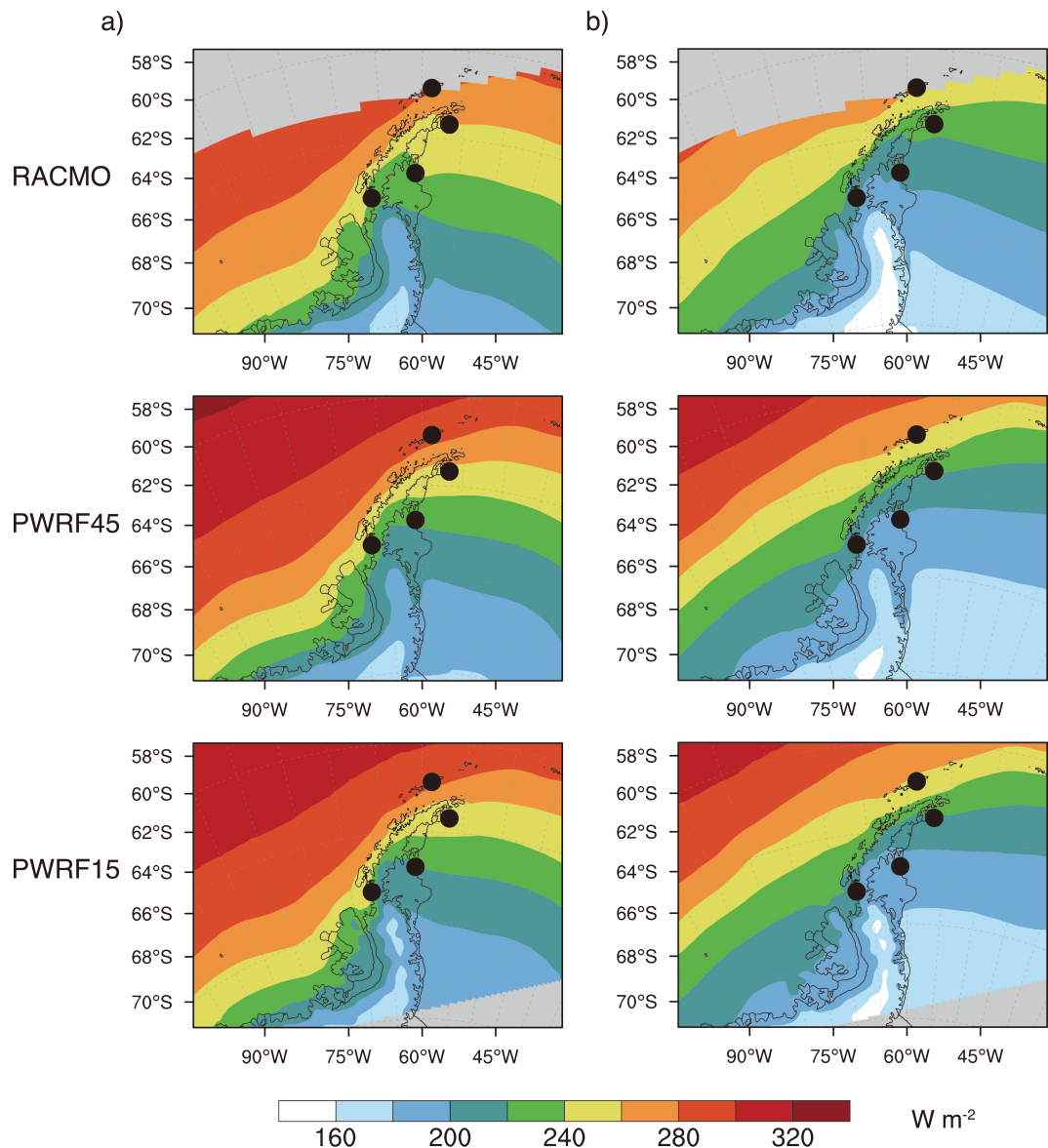


**Fig. S4.** Spatial distribution of mean surface downwelling longwave radiation (1991–2012) over the Antarctic Peninsula for (a) autumn (MAM) and (b) winter (JJA). The filled black circles show the locations of meteorological stations used in this study.

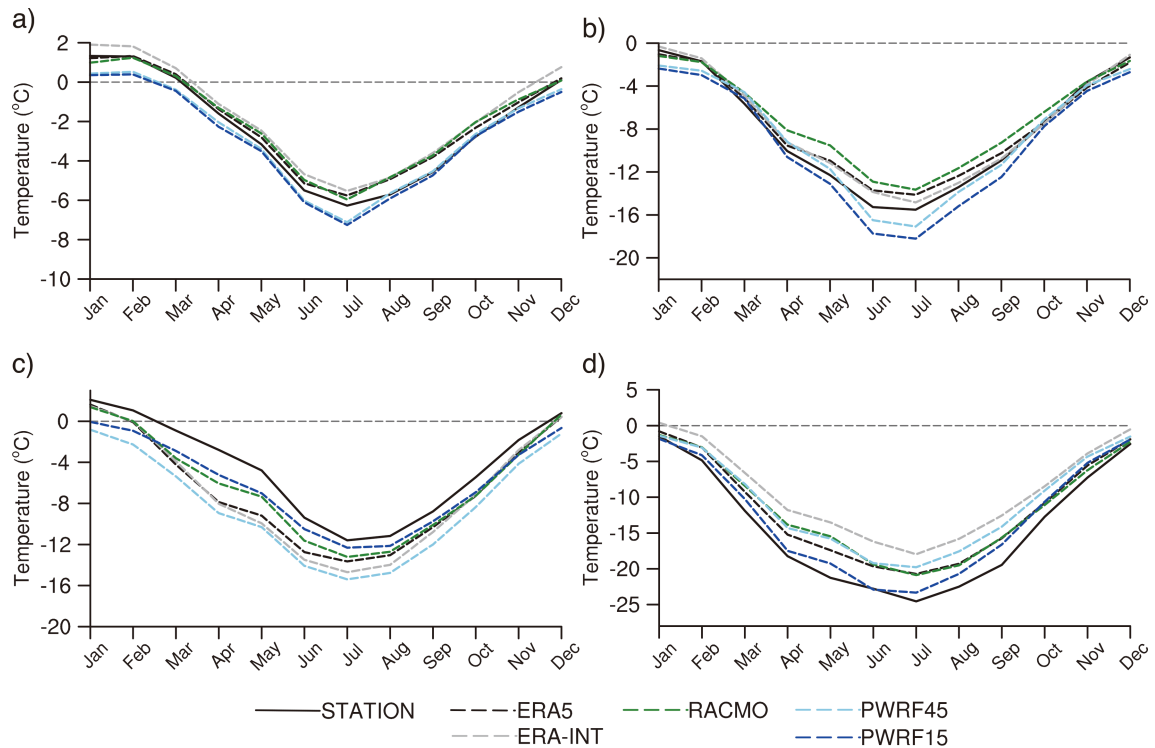


**Fig. S5.** The 22-year (1991–2012) mean annual cycle of near-surface air temperature for the (a) Ed. Frei, (b) Marambio, (c) San Martin and (d) Larsen Ice Shelf stations compared with ERA5 (dashed black line), ERA-Interim (dashed gray line), RACMO (dashed green line), PWRF-45 (dashed light blue line) and PWRF-15 (dashed dark blue line).

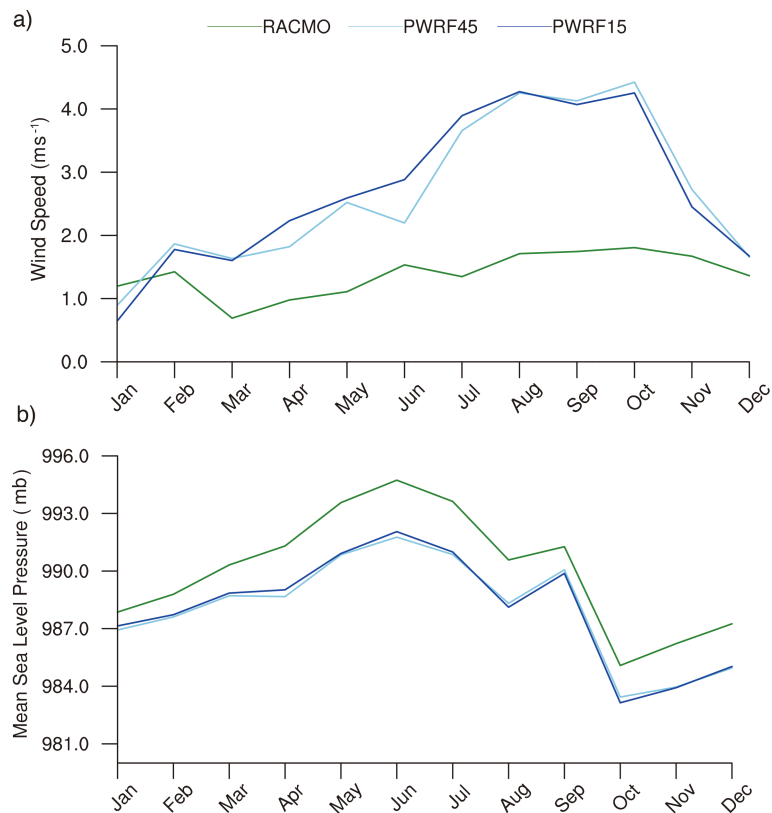


**Fig. S6.** The 22-year (1991–2012) mean annual cycle of (a) wind speed and (b) mean sea level pressure at the grid point of Marambio station for RACMO (green), PWRF-45 (light blue) and PWRF-15 (dark blue).

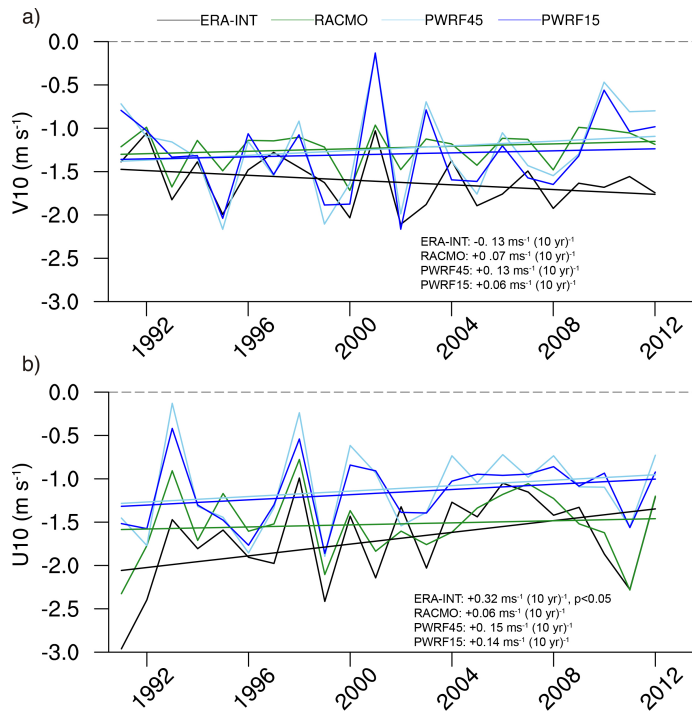
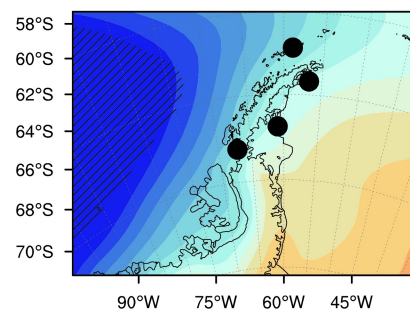
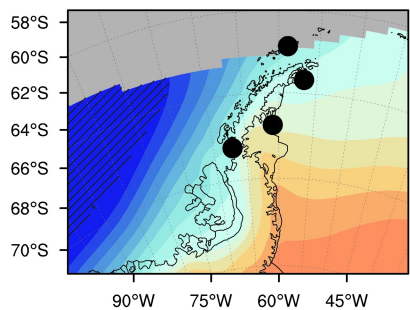


**Fig. S7.** Time series (1991–2012) of summer (DJF) (a) 10-m meridional wind and (b) 10-m zonal wind components averaged over a box covering Alexander Island in the central-southern windward coasts. The black line corresponds to ERA-Interim; green, light blue and dark blue lines are the simulations of RACMO, PWRF-45 and PWRF-15, respectively. Also included are the trend lines for each

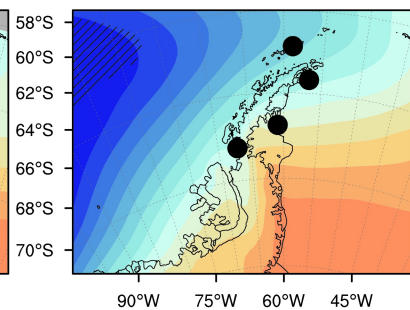
a)



b)



c)



d)

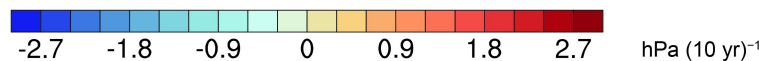
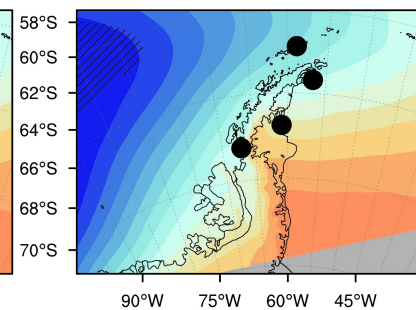


**Fig. S8.** Spatial distribution of autumn (MAM) mean sea level pressure trends (1991–2012) for (a) ERA-Interim, (b) RACMO, (c) PWRF-45, and (d) PWRF-15. The filled black circles show the locations of meteorological stations used in this study. Regions with statistically significant trends at the 95% confidence level based on a two-tailed Student's *t*-test are hatched.

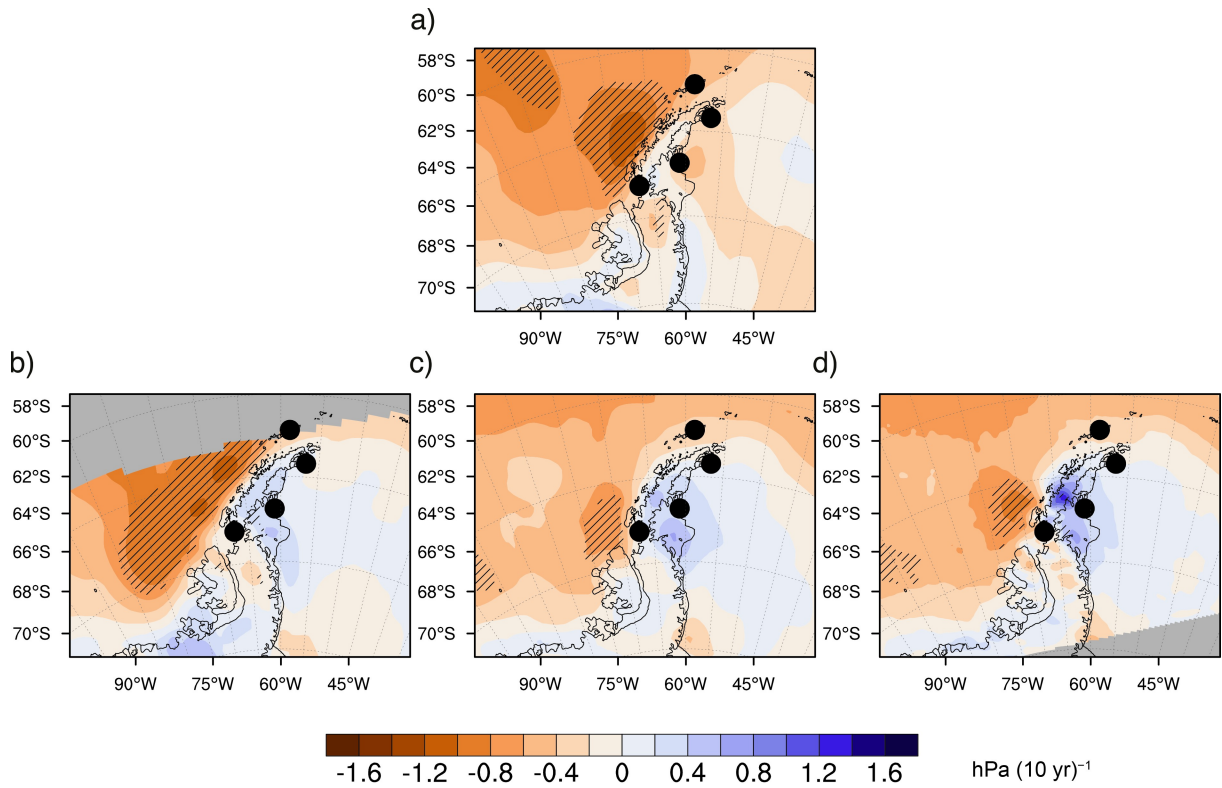


**Fig. S9.** Spatial distribution of autumn (MAM) 10-m meridional wind trends (1991–2012) for (a) ERA-Interim, (b) RACMO, (c) PWRF-45, and (d) PWRF-15. The filled black circles show the locations of meteorological stations used in this study. Regions with statistically significant trends at the 95% confidence level based on a two-tailed Student's *t*-test are hatched.

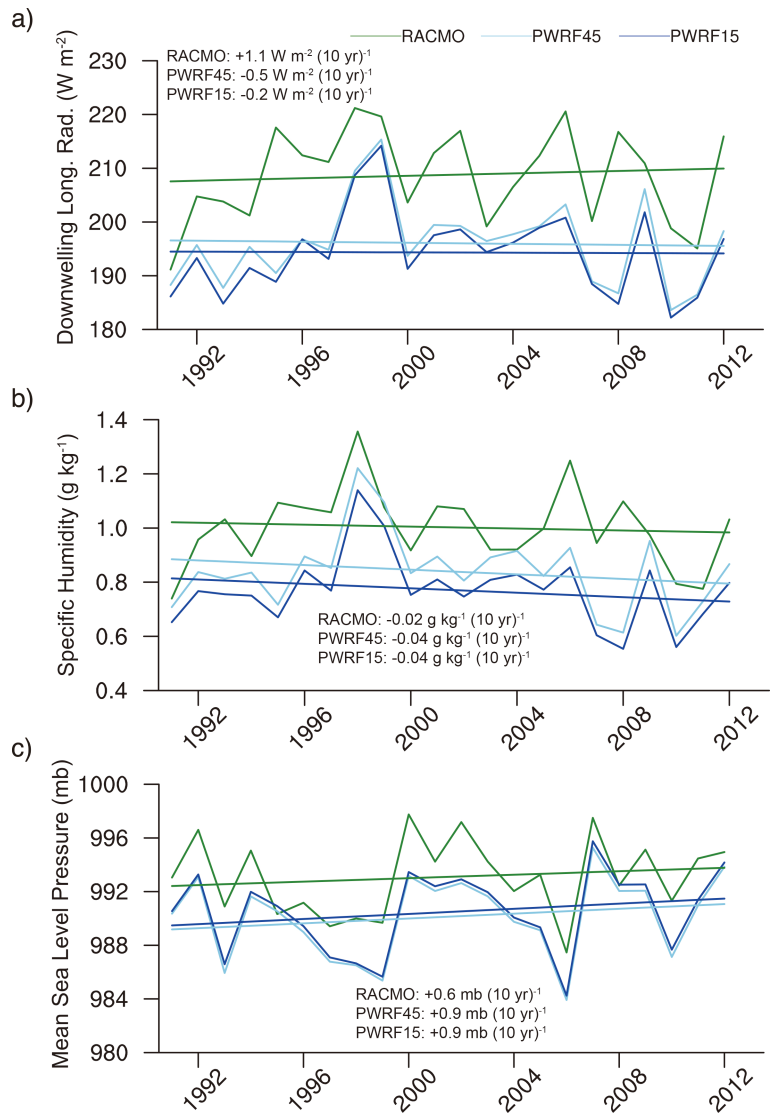


**Fig. S10.** Time series (1991–2012) of (a) surface downwelling longwave radiation, (b) specific humidity at 10 m, and (c) mean sea level pressure averaged over a region in the southeast leeward coasts. Green, light blue and dark blue lines are the simulations of RACMO, PWRF-45 and PWRF-15, respectively. Also included are the trend lines for each time series.